Journal of the Oceanographical Society of Japan
Vol. 32, pp. 53 to 64, 1976

Detailed Observation of the Wind-exerted Surface Flow by Use of Flow Visualization Methods*

Kuniaki OKUDA**, Sanshiro KAWAI**, Masayuki TOKUDA** and Yoshiaki TOBA**

Abstract: Detailed observations were performed of the wind-exerted surface flow, before and after the generation of wind waves. As flow visualization techniques, 6 classes of polystyrene beads of from 0.33 mm to 1.93 mm in diameter, with a specific gravity of 0.99, and also, hydrogen bubble lines, were used. Experiments were carried out at three ranges of the wind speed: 4.0, 6.2 and 8.6 m s^{-1} in the mean in the wind-wave tunnel section, and the observations were made at 2.85 m in fetch. In the case of 6.2 m s^{-1}, when the initial surface skin flow attains 0.22 cm in the scale thickness and 16 cm s^{-1} in the surface velocity in about 3 second from the onset of the wind, regular waves of about 1.7 cm in wave length appear on the water surface. In one second after that, the downward thrust of the surface flow and the consequent forced convection commences, and the transition of the surface layer to a turbulent state occurs. Ordinary wind waves begin to develop from this state. In developed wind waves the viscous skin flow grows on the windward side of the crests, frequently producing macroscopic skin flows, and these skin flows converge to make a downward thrust at the lee side, and the viscous skin layer disappears there. The velocity of the downward flow has a maximum at the phase of about 30°, and the value is of the order of 10 cm s^{-1} at 4-mm depth after the orbital velocity of the sinusoidal wave is subtracted. As the process through which the wind stress acts on the water surface, it is considered that the following particular one may be real: the skin friction concentrated at the windward side of the crest produces skin flows, which thrust into the inner region to make the forced convection, carrying the acquired momentum. The viscous shearing stress just before the generation of the surface undulations was about 1/4 of the total shearing stress under the existence of wind waves. It is considered that the increase of the wind stress by wind waves is caused by this mechanism.

1. Introduction

Phillips-Miles combined instability mechanism for wind-wave generation assumed that the pressure distribution along the water surface was essential for the growth of wind waves (PHILLIPS, 1966). In the treatment of overall rate of the momentum transfer from the air to the water, discussions were sometimes done from a viewpoint of the form drag induced by wind waves, especially of their high frequency components, on the analogy of solid walls (*e.g.*, KRAUS, 1966; IWATA, 1969, 1970; KONDO *et al.*, 1973).

However, efforts of elucidating real processes taking place at the very water surface exerted by wind action have also been continued at the same time. KUNISHI (1957, 1963) observed the growth process of surface flow from the onset of the wind, although the wind speed used was limited to low values. SCHOOLEY (1963, 1971, 1975) studied actual structure of the flow above the surface of wind waves. SHEMDIN (1972), KONDO *et al.* (1974), WU (1975), MCLEISH and PUTLAND (1975) reported measurements of the velocity of wind drift surface current, although their measurements were concerned with horizontally averaged velocity profiles in stationary wind-wave fields. TOBA and KUNISHI (1970) related the breaking of wind waves to the sea-surface wind stress. BANNER and PHILLIPS (1974) and PHILLIPS and BANNER (1974) introduced the wind-induced vortical layer at the surface of the water into the wave dynamics. VALENZUELA (1976) has recently treated the

* Received Aug. 12, 1975, revised Mar. 25 and accepted Apr. 16, 1976.

** Geophysical Institute, Faculty of Science, Tohoku University, 980 Japan

growth of gravity-capillary waves by a model in which shear flows on both sides of the air-water interface are incorporated.

In a recent paper by TOBA *et al.* (1975), a particular flow structure relative to the crests of wind waves has been demonstrated. According to their experimental results, a strong drift current with a considerable shear (the surface skin flow and the macroscopic surface skin flow) exists at the windward side of the crest, within a depth less than the wave height, and the convective downward flow, presumably caused by the convergence of the drift current, is produced at a little lee side of the crest, even though the wind waves are not breaking. Thus the present situation seems to be in a direction that real processes at the air-water interface should further be closely investigated.

From the observation by TOBA *et al.* (1975), we arrived at a concept that real processes of the shearing stress of the wind exerting on the water surface may be mainly the skin friction, under the wide range of wind and wave conditions. Namely, as will be shown in the following sections, the momentum transfer by the skin friction seems to be performed more efficiently under the presence of wind waves. The forced convective structure in water, relative to the crests at any instance of wind waves, suggests that the shearing stress of wind is exerted non-uniformly relative to the wave crests. The stress will act rather concentrically near the crest at the windward side, and it will abruptly intensify the surface skin flow at the windward side. The vertical transfer of momentum will be performed more effectively by the downward convective flow at the lee side of the crest. The mechanism of the momentum transfer near the water surface may thus be quite different from that of the case of solid wall.

A detailed study of these particular phenomena will be essential for the understanding of the transfer process across the air-water interface, not only of the momentum but also of the heat and gases. One of the subjects of the present article is to verify the above described concept of the real process at the wind exerted water surface, through detailed observations of wind-induced surface flow from the onset of the wind to the fully developed state of wind waves. The measurements have been made with a small wind-wave tunnel (15 cm wide and 455 cm long) by use of flow visualization methods. As the tracers, a number of polystyrene small beads of nearly neutral density, and also hydrogen bubble lines have been used. They have been filmed by use of a 16-mm cinecamera and a 35-mm still camera. The detailed description of the experimental methods will also be presented.

2. Wind-wave tunnel and the conditions of the experiment

The experiments have been made with a wind-wave tunnel of 15 cm wide and 455 cm long. A schematic picture is shown in Fig. 1.

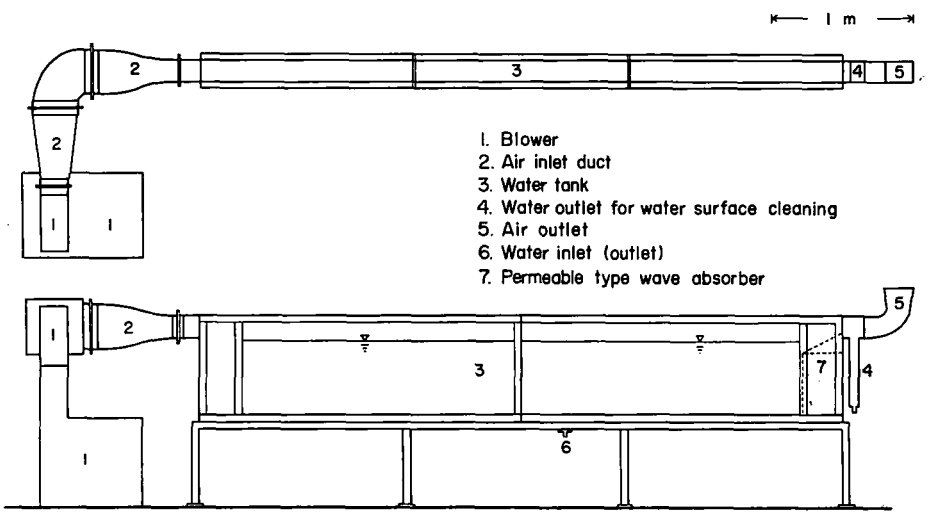

Fig. 1. Schematic sketch of the wind-wave tunnel.

A permeable-type wave absorber is installed at the downstream end of the tank, and a blower at the upstream end. The maximum obtainable wind speed is about 18 m s^{-1} within 17 cm high wind tunnel over 53 cm deep water. For the present study, however, we have used rather low wind speeds from 4.0 m s^{-1} to 8.6 m s^{-1}, since at higher wind speeds the crest of wind wave becomes to be blown off by the wind, which is not the case we intend to investigate in this study. Under this range of wind speed, it is possible to observe the wind waves from 4 cm to 15 cm in wave length at 2.85 m in fetch.

The side walls are made of glass plates so that the observation of the flow is possible from all sides of the tank. In order to remove the surface contamination, the surface water is made overflow the downstream end of the tank by the wind, and removed from a drainage. The cleaning of the water surface is frequently performed in the course of the experiment, since the surface film is likely to be produced in a rather short period of several hours. In our observation, when the water surface is filmed by the contamination, growth of the surface skin flow is hindered until the surface contamination is drained off.

Wind profiles were measured by use of a pitot-static tube and a manometer. Examples measured at 2.85 m in fetch are shown in Fig. 2. The turbulent boundary layers have developed up to a height of about 5 cm above the mean level of the interface, and the shearing stress of the wind was calculated from the logarithmic wind profiles. The wave height and the period of wind waves were measured by use of capacitance probes. In Table 1 are summarized the characteristic values with respect to wind and wind waves in the present experiment.

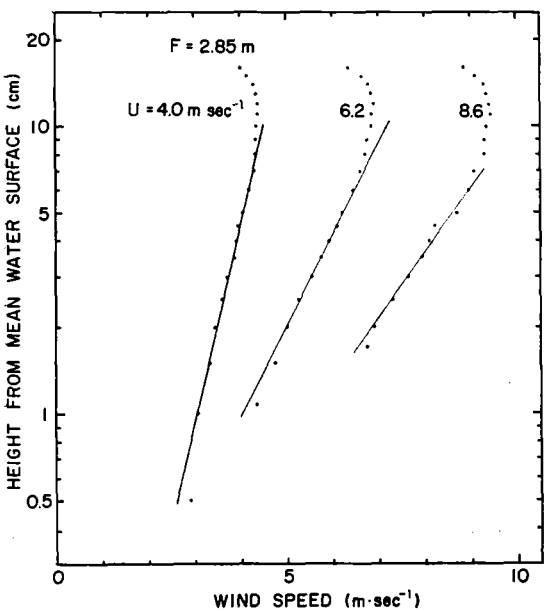

Fig. 2. Examples of the wind profile measured at the center of the tunnel in the cross-wind direction at 2.85 m in fetch.

It should be noted that the surface skin flow and the forced convection, on which our attention is placed, may be essential factors in the phenomena at the water surface exerted by the shearing stress of wind. They have the same order of magnitude of velocity near the interface as the orbital motion of wind waves. The results obtained using this small tank will have a sufficient applicability to the oceanic phenomena, in their essential features of physical importance.

3. Flow visualization

The neutral beads and the hydrogen bubble lines were illuminated by a stroboscope which emitted pulses of light at a desired frequency, or the external triggering by a camera shutter. To reduce the halation at the upper side of the interface, the stroboscope was set so that the flashing-light is injected into the water nearly perpendicularly to the interface.

The tracers were filmed by a cinecamera for the determination of flow velocity, and also by a 35-mm still camera auxiliary for the qualitative investigation. The exposed time of each frame

Table 1. Summary of characteristic values of the present experiments.

	Case 1	Case 2	Case 3
Wind speed (cm s^{-1})			
Average in the tunnel section	4.0	6.2	8.6
Extrapolated to 10-m level	7.1	12.8	17.9
Wind stress (dyn cm^{-2})			
Estimated from wind profile above developed wind waves	0.62	2.96	5.76
Friction velocity u_* (cm s^{-1})	22.8	49.6	69.2
Developed wind waves			
Characteristic wave period T(s)	——	0.23	0.27
Average wave height H(cm)	——	0.94	1.74
Fetch of observation (m)	2.85	2.85	2.85

from the onset of wind was known by the record of the flushed time using a circuit of photo-transistor. The sharp-cut images of tracers were taken, since each flashing-time was 20 microseconds, so that the movements of the tracers during the exposure were negligible.

3.1. Polystyrene beads

In order to trace the movement of water particles, a large number of polystyrene beads smaller than 2 mm in diameter may be used after some treatment. The preparation is as follows. The density of the beads is originally about 1.04 g cm^{-3}. They are dipped in water in a beaker, and heated by adding some hot water slowly. The beads foam and become opaque, and as soon as some of them become to rise up by buoyancy, the heating is stopped. Then particles of the neutral density are sorted and collected by suspending them in a large container of water.

Some examples used through the experiments are shown in Fig. 3. It was taken from a viewpoint slightly below the air-water interface, and the beads were filmed coupled with the reflections from the underside of the interface. Their density is slightly smaller than that of water but very close to it, because all of them are touching the interface at points and are seen almost completely as spheres. The mean specific gravity of the beads used was 0.99 which was measured by use of a specific-gravity bottle.

A further treatment was added to use them effectively in our experiment. Since the surface of the beads is slightly hydrophobic, they may rise through water by the attachment of small air bubbles, or they hardly submerge into water by the effect of surface tension when they contact the air-water interface. However, the problem was settled by a rather unexpected manner by putting a kind of dye on their surface. This method was found when they were colored in order to be distinguished easily on 16-mm color film. The surface of the colored beads became wet completely at the instance they were dropped in water, and never caught air bubbles in the course of the experiment.

They were used to calculate the flow pattern relative to the crest of wind wave. We prepared several tens thousands of neutral beads for this purpose, since it was necessary to distribute them with sufficient density in the tank, in order that at least several tens of beads were included in each picture of about the wavelength wide. Further, they were classified into six groups by their size, for a particular purpose to observe the growth process of the surface skin flow. The velocity profile near the interface was determined at every moment from the onset of wind, regarding the velocity of the beads with various diameters as the flow velocity at the depth of their radius, or at the center of the beads. This method of using the difference of diameters of spherical particles, to obtain the velocity profile near the interface, is the same as that used by WU (1968) who examined the mean velocity profile under the developed wind waves. A sample of our beads is shown in Fig. 4. The mean diameter of each group was 1.93, 1.53, 1.03, 0.73, 0.53 and 0.33 mm, respectively, and the maximum variation was less than 0.05 mm for each group. Further, in order to make the size distinction on the 16-mm cine-pictures easy, the groups were dyed alternatively blue and green.

3.2. The bubble lines

The other tracer is hydrogen bubble lines produced by the electrolysis of water. A 50-micron platinum wire was stretched vertically through the interface, and DC electrical pulses were provided by a pulse generator, which could act at 1 to 100 pulses s^{-1}, or by external triggaring by a camera shutter. The size of produced bubbles, or consequently their ascent velocity in water, was controlled by changing the pulse width. The pulse generator was operated at the narrowest pulse width as far as the bubbles were clearly filmed, since the velocities determined from the trace of rising bubbles are depth averaged in the interval of buoyant rise, and then the calculated velocity profile may be rather smoothed. We operated it at 2 milliseconds for which the bubbles with ascent velocity of about 0.91 cm s^{-1} were produced.

In Fig. 5, which will be discussed in detail in the next section, is shown the bubble lines produced at 0.04-s intervals. The instantaneous velocity profile may be determined from the movement of each line in a time of exposure interval of 16-mm cinecamera. This method is quite efficient when the flow is laminar, but it

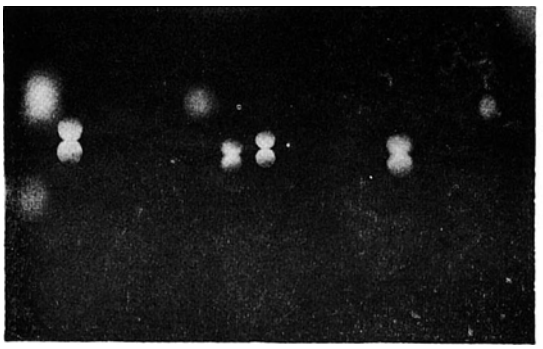

Fig. 3. The polystyrene beads of the specific gravity of 0.99, used for the measurement of surface flow. They are in contact with the interface at their tops.

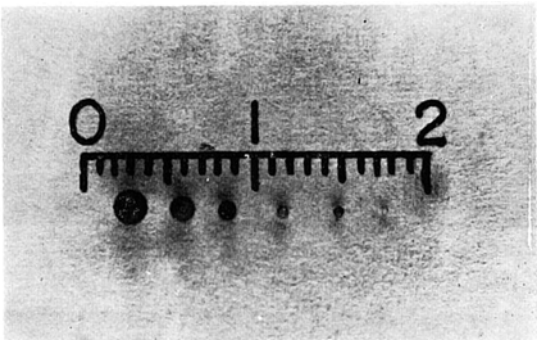

Fig. 4. The classified polystyrene beads. The diameters are 1.93, 1.53, 1.03, 0.73, 0.53, and 0.33 mm, from the left. The scale in the picture is in centimeters.

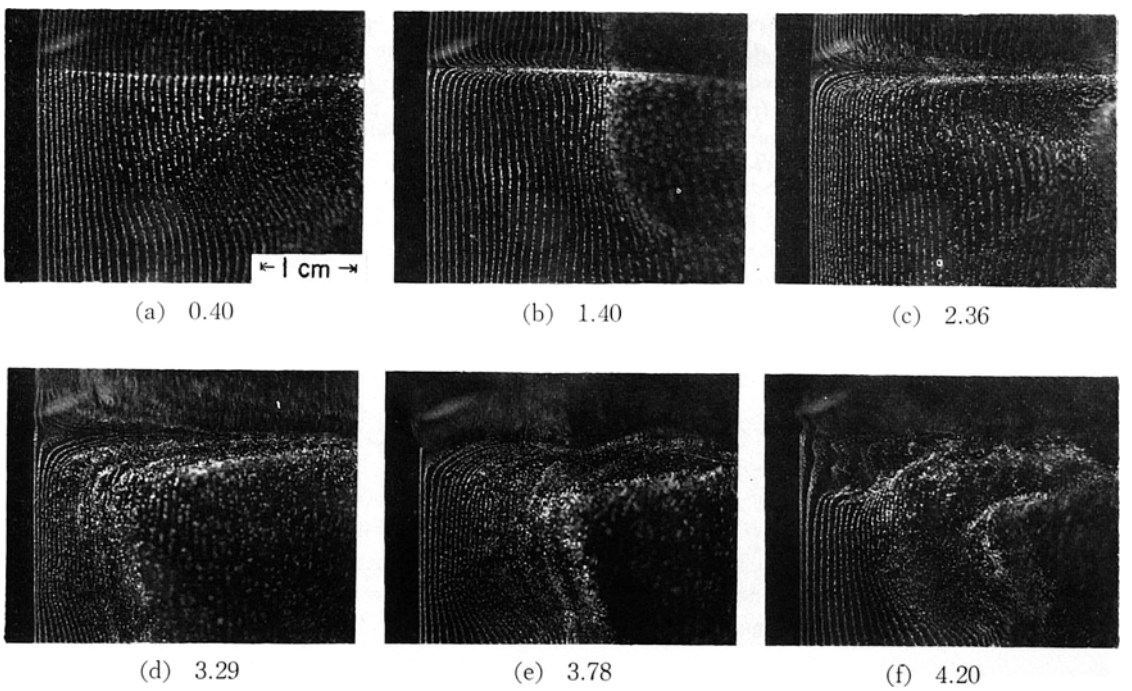

Fig. 5. Growth process of the surface skin flow observed by use of the hydrogen bubble lines produced by the electrolysis of water. The electrical pulses of 0.002-s width were provided at 0.04-s intervals. The wind was blowing from the left to the right of each picture at 6.2 m s^{-1}. A weak mean flow was produced previously before the onset of wind. The filmed time of each picture from the onset of wind is shown by seconds. The photographs were taken from a viewpoint slightly below the air-water interface. Images reflected at the interface are seen in the upper part of the pictures. The out-of-focus area was caused by some fluctuation of the mean flow.

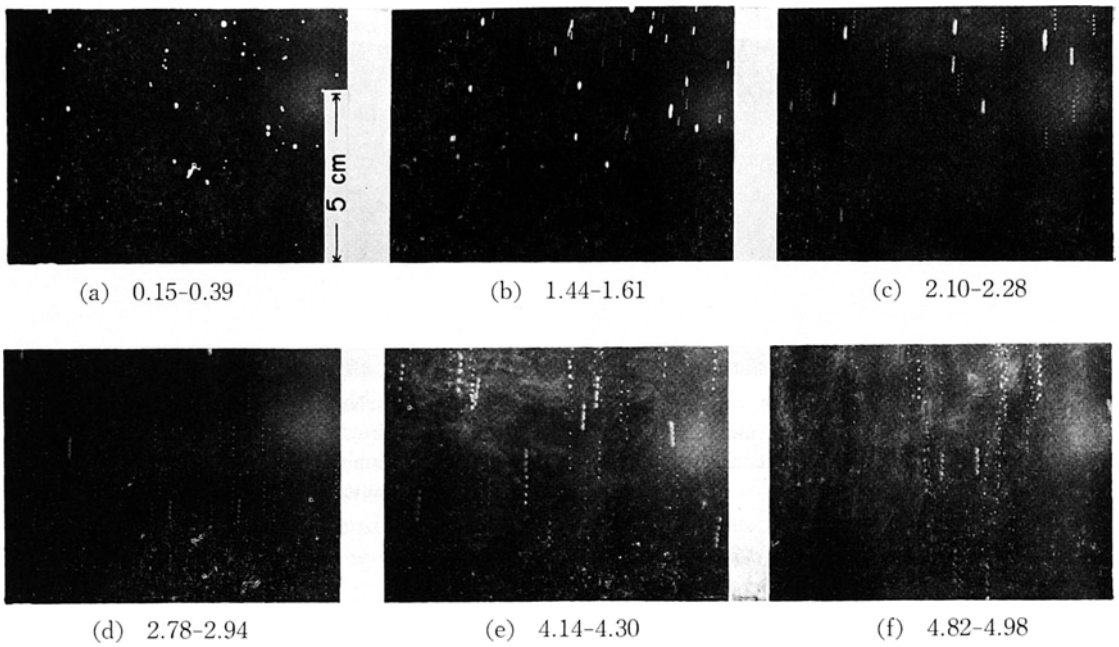

Fig. 6. Growth process of the surface skin flow observed by use of the classified polystyrene beads. The shutter speed was set at 1/8 s, and the pulse of light was provided at 40 Hz. The wind was blowing from the bottom to the top of each picture at the same speed with that of Fig. 5. The figures shown at the bottom of each picture shows the time of shutter opening and closing in second from the onset of the wind

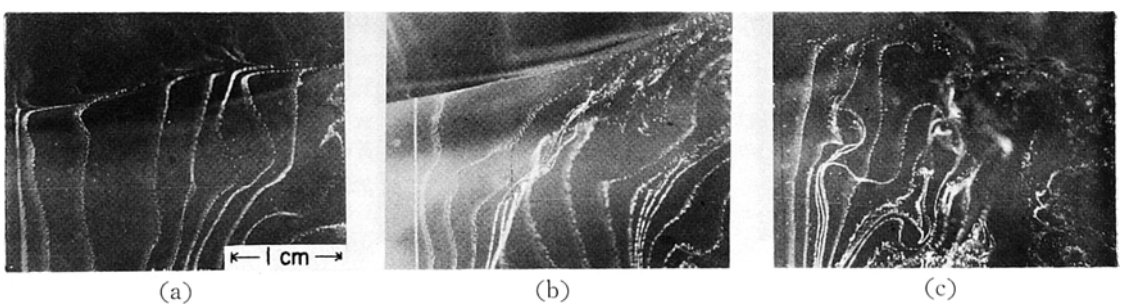

Fig. 8. The flow pattern beneath the interface under the representative wave crests. The wind was blowing from the left to the right of the pictures at the same speed with that of Fig. 5. (a), (b): Flow pattern at the windward side of the crest. The surface skin flow is seen clearly in (a), and the macroscopic surface skin flow in (b). (c): Flow pattern at the lee side of the crest. The convective turbulence is likely to exist to the depth of about 1.5 cm from the interface.

should be used rather carefully in a turbulent flow, since in this case, the vertical movements of each bubble may not be traced correctly from the ascent velocity only. The surface flow in the wind wave field is turbulent, and especially strongly so at the lee side of the crest, where the downward flow is produced. Thus, we used this method for the determination of the velocity profile at the restricted region relative to the crests of wind wave, where the turbulence was rather weak. The surface flow beneath the interface at the windward side was determined by this method, while the convective turbulence at the lee side was by the neutral particle method.

4. Results of the experiments

4.1. Growth process of surface skin flow

The surface skin flow just after the onset of wind was observed, under three wind speeds, by use of the classified neutral beads and hydrogen bubble lines. In Fig. 5 is shown a series of pictures of hydrogen bubble lines, taken under the wind speed of 6.2 m s^{-1} in an average in the tunnel section. Before the onset of the wind, a weak mean flow was intentionally produced, and the bubble lines were emitted at 0.04-s intervals. Diffused lines in the upper side are the reflections from the underside of the air-water interface. The flow just after the onset of the wind was completely laminar as seen in the sequential photographs of Fig. 5 (a, b, c, d and e). The thickness as well as the velocity of the flow increases by the molecular diffusion of momentum, as investigated by KUNISHI (1957, 1963) at lower wind speeds. As the laminar surface flow develops, the surface undulation becomes to be appreciable (Fig. 5(e)). The wavelength, seen in the picture, is about 1.7 cm. The manner of its growth is quite regular, in contrast to that of wind waves in later stages. At first, several groups of distinguishable crests, each of the group consisting of more than 5 or 6 crests, are found in some region near the center of the tunnel in the cross-wind direction. They grow rather abruptly and, at the same time, fresh crests successively appear on the adjacent level water surface. In about 0.8 s, they become to be distinguishable almost everywhere. The distances between neighboring crests are nearly uniform, and change little in their growth process. The surface flow remains laminar untill they grow to some extent. The successive pictures of 16-mm film taken at 42 frames s^{-1} suggest that, when the steepness approaches to about 0.1, the surface skin flow of a thickness of several millimeters suddenly changes to turbulent state by downward thrust of surface water in one or two frames, that is, in a quarter or a half of the undulation period. The regular undulation collapses on the commencement of this turbulence, and the interface becomes irregular. It seems that the growth of wind waves, accompanied by the increase in wavelength, begins just after that, and the turbulent nature of the surface flow reaches rapidly to deeper region by the induced convective turbulence (Fig. 5(f)). KUNISHI (1957, 1963) suggested that a conspicuous vortex, extending through the whole layer of laminar surface flow, sporadically occurs just before the initial growth of surface undulations. His result differs from ours, however, the discrepancy will be attributed to the difference of wind conditions: Kunishi's experiments were made at much lower wind speeds.

The velocity gradient near the interface was measured by use of the classified beads. The analysis of the velocity has been performed using pictures taken by a 16-mm cinecamera which was directed perpendicularly to the interface. However, a series of stroboscopic pictures taken by a 35-mm still camera is shown here to demonstrate the possibility of this method, although only positive cinefilms were used for the analysis through the experiments. The pictures in Fig. 6 were taken at the same wind speed with Fig. 5; the shutter speed was set at 1/8 s, and the pulse of light was at 40 Hz. The wind was blowing from the bottom to the top of the pictures. The flow velocity was easily obtained from a distance between successive images of each bead divided by 1/40 s. The cloudy white regions in (e) and (f) of Fig. 6 are the tracks of the undulation. In the course of the experiment, none of the beads protruded on the water surface, and the beads were distinctly filmed without any halation. The errors contained in the velocity gradient evaluated by this method will solely be due to the variability of diameters in each size group of beads, thus the maximum errors may be estimated easily

as ±6%. By use of this method the velocity gradient near the interface was determined for three cases of the wind speed. The observed characteristic values of the surface skin flow just before the generation of wind waves are summarized in Table 2.

In Fig. 7 is shown the growth process of the surface skin flow. The velocity profiles were calculated successively from the onset of wind until the beads became to be entrained into the inner region of water by the commencement of convective turbulence. The beads of 0.53 mm were not used, in this case, to make the size

Table 2. Characteristic values of the surface skin flow just before the generation of wind waves.

	Case 1	Case 2	Case 3
Average wind speed above developed wind waves ($m\,s^{-1}$)	4.0	6.2	8.6
Scale thickness of surface skin flow layer (cm)	0.29	0.22	0.14
Estimated surface velocity ($cm\,s^{-1}$)	12.2	16.2	16.4
Wind stress estimated from shear of surface skin flow before generation of wind waves ($dyn\,cm^{-2}$)	0.42	0.74	1.14

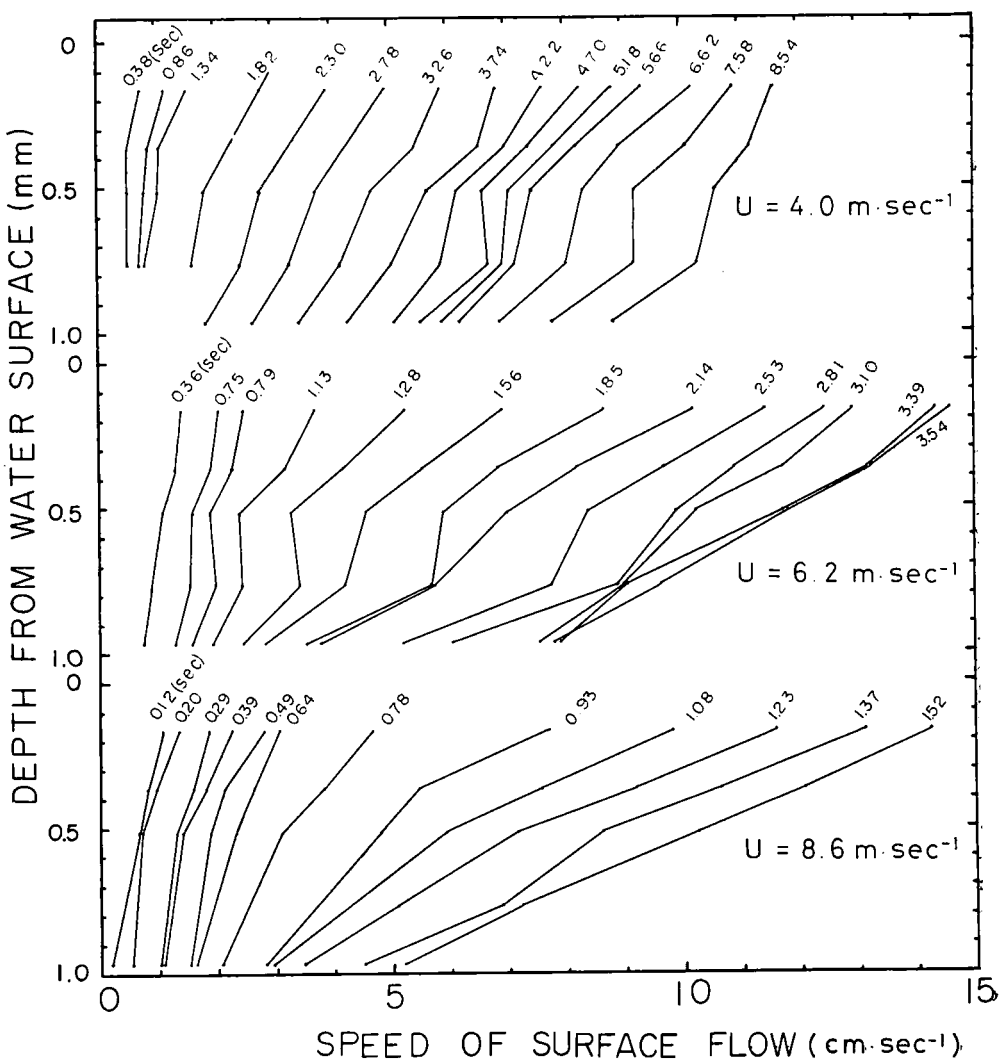

Fig. 7. Velocity profiles of the surface flow in the laminar state. The measurements were made by using neutral beads method at 2.85 m in fetch. At each wind speed, the velocity profiles from the onset of wind to just before the commencement of turbulence are shown.

distinction easy. The instantaneous velocities of about ten beads in each size group were averaged to obtain the flow velocity at respective depth. The velocity profiles just before the commencement of turbulence may be approximated by linear functions of the depth. The skin friction calculated from them are 0.42, 0.74 and 1.14 dyn cm^{-2} at 4.0, 6.2 and 8.6 m s^{-1} wind speeds, respectively. These values are much smaller than that estimated from the mean wind profiles which were obtained over the fully developed wind waves. The shearing stress of wind obtained from Fig. 2 is 0.62, 2.96 and 5.76 dyn cm^{-2} for the three wind speeds, respectively. These results suggest that the shearing stress of wind increases very much through the growth process of wind waves. The increased wind stress, however, is not necessarily considered as that transported to water through the form drag by the surface irregularity of wind waves. The observation of surface skin flow under developed wind waves, as shown in the next section, suggests that the skin friction is also intensified considerably by the growth of wind waves.

The thickness of the surface skin flow should be mentioned here for comparison with the case of developed wind waves. It increases from the onset of wind and reaches a maximum just before the commencement of turbulence, then the layer becomes much thinner, since the turbulence successively destroys it. The scale thicknesses just before the commencement of turbulence, under the three wind speeds, were 0.29, 0.22 and 0.14 cm, respectively, the calculation being made at 8.5, 3.5 and 1.5 seconds from the onset of wind. The surface velocities at the respective times, obtained by extending the velocity profiles linearly to the water surface, were 12.2, 16.2 and 16.4 cm s^{-1}, respectively.

4.2. Turbulent structure in the wind wave field

In the developed wind wave field, the surface flow is strongly turbulent, and the layer of the surface skin flow is much thinner than in the state before the commencement of turbulence. The turbulent structure in the surface layer is characterized by the downward flow produced at the lee side relative to the crest of wind wave, as reported by TOBA *et al.* (1975) as the forced convection.

In Fig. 8 is shown examples of the flow pattern beneath the interface in the wind wave field. The wind speed was 6.2 m s^{-1}, and blowing from the left to the right in the pictures. The water surface may be distinguished as a crossing point of bubble lines and their rather diffused reflections at the underside of the interface. At the windward side of the crest, the surface skin flow with a great shear exists within a depth of less than 1 mm (Fig. 8(a)). The flow was seen certainly in most of the pictures taken at the windward side, but the thickness varied considerably. The mean thickness was calculated, from pictures in which the surface skin flow was surely distinguished, as 0.46 mm. For pictures taken near the peak of the crest, the thickness was much thinner and our method was not able to resolve it exactly. The above value is one order of magnitude smaller than that obtained by WU (1968) as a mean value through the passages of several crests under similar wind speed. On this point, it is considered that WU observed much thicker shear flow frequently found in our pictures, *e.g.* as Fig. 8(b).

In Fig. 8(b), the shear flow which is clearly distinguished from surface skin flow is seen to a depth of about 0.5 cm. The flow, which has been called "macroscopic surface skin flow" by TOBA *et al.* (1975), has usually a considerable shear. However, the velocity often becomes rather uniform near the interface, and in this case it rapidly decreases at a depth of about 0.5 to 1.0 cm, producing there a great shear. The successive pictures of 16-mm film suggest that the flow is distinguished only at the windward side of the crest; it seems to be exhaustively dissipated at the lee side where the convective downward flow is produced. Since the intensity and the profile seem to vary considerably whenever we observe, it is plausible that it is influenced almost directly by the turbulent fluctuations of shearing stress of wind.

Fig. 8(c) shows a condition of the flow field at the lee side of the crest. The bubble lines are entangled or rather broken into many pieces of bubble clouds down to a depth of about 2 cm, the condition being quite different from that of windward side. The phenomenon is not the breaking of wind waves in a usual

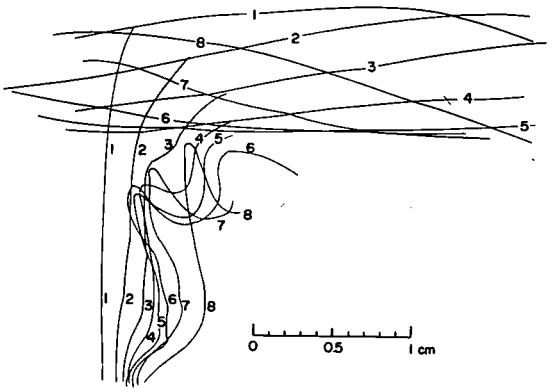

Fig. 9. The trace of a bubble line in the passage of a representative wave trough. The wind was blowing from the left to the right at 6.2 m s^{-1}. The bubble line was followed from 1 to 8 at 1/35.7-s intervals. The configuration of the air-water interface at the respective time is shown in the upper part.

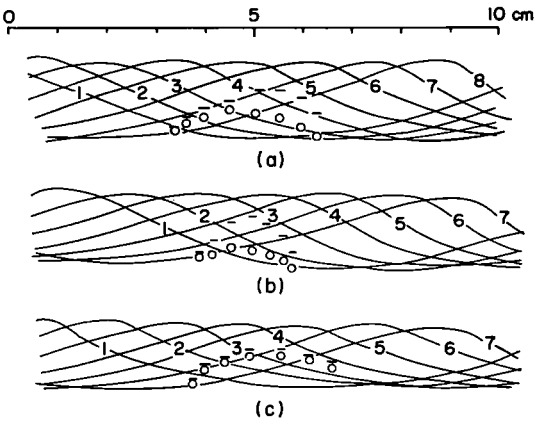

Fig. 10. Some examples of the movement of neutral beads in the passage of a representative wave crest. The wind was blowing from the left to the right at the same speed with that of Fig. 9. The beads were traced from the left to the right at 1/42-s intervals, and the configurations of water surface at the nearer wall of the tank at the corresponding times are shown in the upper part. The bars (−) represent the corrected position of the water surface just above each bead.

sence, since the entrainment of air bubbles never occurred through the process in the above described range of our experiment.

A bubble line was traced at 1/35.7-s intervals in the passage of a wave trough by successive pictures of 16-mm film (Fig. 9). It was emitted near the position marked by 1, and followed to 8; the configuration of the interface at each time is shown in the upper part with the corresponding number. The wavelength and wave height seen in the figure were about 8 cm and 0.8 cm, respectively, under 6.2 m s^{-1} wind speed. The strong downward flow is seen at the lee side (5-8), and rather weak upward flow is likely to exist at the windward side (1-5) to a depth of about 1 cm. Similar flow pattern is found in almost all pictures taken under various wind speeds. The surface layer under wind wave field thus seems to have a turbulent structure characterized by the convective downward flow at the lee side relative to the representative wave crest, even if the breaking of wave crest is not occurring as pointed out by TOBA *et al.* (1975).

The evaluation of velocity of such a convective turbulence has been made using the polystyrene beads method. Some traces of the neutral beads in the passage of a crest are shown in Fig. 10. The wind is blowing from the left to the right at the same speed with Fig. 9. Successive positions of each bead and the configuration of the interface were followed at 1/42-s intervals from the left to the right. In the pictures, the interface has been filmed with some width, since the camera was directed from a view point slightly below the interface. The line of the interface was drawn in the figure at the near wall of the tank, thus the depth of each particle must have been measured from a point a little below it. The determination of the point was made with such a manner that may have been considered least optional. In the determination of velocity near the interface, only the beads which remained in focus through the passage of a crest were selected, and their movement in the cross-wind direction was assumed to be small in the period considered. The location of the beads in the cross-wind direction was determined by knowing the proportion of the distance of the beads from the nearer wall of the tank to the total width of the interface, from the pictures in which the position of the beads could easily be identified by the reflections at the interface. In Fig. 10, the bar (−) indicates the point on the interface just above the bead, determined by such a manner.

The downward flow at the lee side and the upward flow at the windward side are also seen in (a) and (b) of Fig. 10. This turbulent structure is more clearly shown by extracting the velocity induced by the surface undulation. Most simply, it may be made by assuming the wind wave as a sinusoidal wave with the wavelength and the amplitude determined from the pictures. The velocity of the convective downward flow thus obtained amounted 10.8 cm s^{-1} at the depth of 4.0 mm in case (a), and 9.3 cm s^{-1} at 4.2 mm in case (b). The values were calculated at the phase of about 30° before the peak of the crest, where the downward flow seems to have the maximum value.

Some of the beads were not entrained into the inner region of water (Fig. 10(c)). The fact may indicate that the downward flow is much weaker at just beneath the interface compared with a little inner region, thus even if the beads have an only slightly smaller density than that of surrounding water, they will hardly be entrained into water. It is also probable that the intensity of the convection is rather variable, although it occurs at almost every crests as mentioned before. It seems, however, that the convective turbulence has the same order of magnitude of intensity with the orbital motion of representative wind waves, although some statistical treatment must be needed to exhibit the characteristics quantitatively well. It may be noted that this phenomenon is different from that investigated by BANNER and PHILLIPS (1974), in which they suggested that the breaking of short gravity waves is considerably accelerated by the existence of surface drift. In our observation, in spite that there was no breaking of waves, the convective turbulence did occur. Also, the flow velocity near the interface at the peak of the crest did not usually exceed the phase velocity, and when it occurred, it was restricted in the surface skin layer thinner than 1 mm in thickness. Concerning characteristic gravity waves, it does not seem possible that the skin flow directly maintain the convective turbulence which almost always exists relative to the crest of wind wave to a depth of more than 1 cm.

The convective turbulence appears as a jet produced by the continuous downward thrust of water near the interface. It seems that the surface flow, particularly the macroscopic surface skin flow, converges there as suggested by TOBA *et al.* (1975). If the separation of the air flow is occurring on the trough region as observed by SCHOOLEY (1963), and the greater part of the shearing stress of wind acts on the water surface around the crest, the surface flow will concentrically be intensified near the peak of the crest and induce the convergence at the lee side.

More closely speaking, the process seems to be plausible considering the fact that the surface skin layer near the peak of the crest is much thinner than in other regions. The shearing stress of wind may act there very strongly by the skin friction, and must be transported into inner region of water rapidly. The small scale convective turbulence, as mentioned before on the commencement of turbulence, must also be occurring under the crests of shorter waves riding over the crests of representative gravity wave. Consequently, the intensity of turbulence just below the interface may be sufficiently strong. The momentum aquired at the water surface may be successively transported, by such small scale convective turbulence to a depth of several milimeters, and as a result, the macroscopic surface skin flow may be produced at the windward side of the crests to induce the convergence at the lee side.

Verification of the process with a more severe quantitative manner is now undertaken. However, the intensity and the scale of the convective turbulence are possibly explained as the convergence of the macroscopic surface skin flow. It may be said that a considerable part of the shearing stress of wind is accumulated as the macroscopic surface skin flow near the interface, especially near the crest at the windward side, then it is transported into the inner region of water by the strong convective downward flow especially at the lee side of the crest. The macroscopic surface skin flow and the convective turbulence relative to the crests of wind waves thus seem to form a unique transfer process of momentum at the air-sea interface. This process is quite different from that on the solid boundary. A quantitative evidence of the variable distribution of the shearing stress along the wave profile will be reported in a subsequent paper.

References

BANNER, M.L. and O.M. PHILLIPS (1974): On the incipient breaking of small scale waves. J. Fluid Mech., **65**, 647-656.

IWATA, N. (1969): Aerodynamic roughness of the sea surface. La Mer, **7**, 269-277.

IWATA, N. (1970): A complementary note on the aerodynamic roughness of wind disturbed sea surface. La Mer, **8**, 240-245.

KONDO, J., Y. FUJINAWA and G. NAITO (1973): High-frequency components of ocean waves and their relation to the aerodynamic roughness. J. Phys. Oceanogr., **3**, 197-202.

KONDO, J., G. NAITO and Y. FUJINAWA (1974): Wind-induced current in the upper most layer of ocean. Natl. Res. Center for Disas. Prev., Rept., No. 10, 67-82 (in Japanese).

KRAUS, E.B. (1966): The aerodynamic roughness of the sea surface. J. Atmos. Sci., **23**, 443-445.

KUNISHI, H. (1957): Studies on wind waves with use of wind flume (I), —On the shearing flow in the subsurface boundary layer caused by wind stress—. Ann. Disas. Prev. Res. Inst., Kyoto Univ., **1**, 119-127 (in Japanese).

KUNISHI, H. (1963): An experimental study on the generation and growth of wind waves. Disas. Prev. Res. Inst., Kyoto Univ., Bull., No. 61, 41pp.

MCLEISH, W. and G.E. PUTLAND (1975): Measurements of wind-driven flow profiles in top millimeter of water. J. Phys. Oceanogr., **5**, 516-518.

PHILLIPS, O.M. (1966): The Dynamics of the Upper Ocean. Cambridge Univ. Press, London, 261 pp.

PHILLIPS, O.M. and M.L. BANNER (1974): Wave breaking in the presence of wind drift and swell. J. Fluid Mech., **66**, 625-640.

SCHOOLY, A.H. (1963): Simple tools for measuring wind fields above wind-generated water waves. J. Geophys. Res., **68**, 5497-5504.

SCHOOLY, A.H. (1971): Diffusion sublayer thickness over wind-disturbed water surfaces. J. Phys. Oceanogr., **1**, 221-223.

SCHOOLY, A.H. (1975): Simple method for measuring relative humidity, water and air temperatures within a few millimeters of wind-generated water waves. J. Phys. Oceanogr., **5**, 519-522.

SHEMDIN, O.H. (1972): Wind-generated current and the phase speed of wind waves. J. Phys. Oceanogr., **2**, 411-419.

TOBA, Y. and H. KUNISHI (1970): Breaking of wind waves and the sea surface wind stress. J. Oceanogr. Soc. Japan, **26**, 71-80.

TOBA, Y., M. TOKUDA, K. OKUDA and S. KAWAI (1975): Forced convection accompanying wind waves. J. Oceanogr. Soc. Japan, **31**, 192-198.

VALENZUELA, G.R. (1976): The growth of gravity-capillary waves by the coupled-shear flow model. J. Fluid Mech., (in press).

WU, J. (1968): Laboratory studies of wind-wave interactions. J. Fluid Mech., **34**, 91-111.

WU, J. (1975): Wind-induced drift currents. J. Fluid Mech., **68**, 49-70.

流れの可視化法を用いた風による表面流の詳細な観察

奥田邦明* 河合三四郎* 徳田正幸* 鳥羽良明*

要旨：風波発生前後における風による表面流を詳しく観察した．流れの可視化には直径 0.33 ないし 1.93 mm の 6 つのクラスの，比重 0.99 のポリスチレン粒子，および水素気泡列を用いた．実験は，風洞水槽における断面風速 4.0, 6.2, 8.6 m s^{-1} の 3 段階で行い，主として吹送距離 2.85 m で観測した．6.2 m s^{-1} のときには，風が吹き始めるとすぐに皮流が発生し，それは約 3 秒で厚さ 0.22 cm，表面流速 16 cm s^{-1} に達し，約 1.7 cm 波長の規則的なでこぼこが水面に生じる．その後 1 秒のうちに皮流が下向きに突っ込む強制対流が始まり，表層は乱れた状態に移行し，ふつうの風波はその状態から発達する．発達した風波では，皮流は峯の風上側に発達し，しばしばマクロな皮流となり，風下側ではその収束で下降流が生じ，表層の分子粘性層は消滅する．下降流は，峯のピークから 30° 程度前面で最大で，波の軌道運動の速度をさしひくと，水面下 4 mm で 10 cm s^{-1} の程度である．風の運動量は，波の峯の風上側に集中した接線応力が皮流を生じ，それが峯の前面で収束して下に突っ込むという特殊な過程を通して水に輸送されていると考えられる．風波発生直前の分子粘性による応力は，風波存在下の水面応力の 1/4 であった．風波による水面応力の増大は，この機構によって生じていると思われる．

* 東北大学理学部地球物理学教室，〒980 仙台市荒巻字青葉